Caspases as Key Executors of Methyl Selenium-induced Apoptosis (Anoikis) of DU-145 Prostate Cancer Cells[1]

Cheng Jiang, Zaisen Wang, Howard Ganther, and Junxuan Lu[2]

AMC Cancer Research Center, Denver, Colorado 80214 [C. J., Z. W., J. L.], and University of Wisconsin-Madison, Madison, Wisconsin 53706 [H. G.]

ABSTRACT

Apoptosis induction may be a mechanism mediating the anticancer activity of selenium. Our earlier work indicated that distinct cell death pathways are likely involved in apoptosis induced by the CH_3SeH and the hydrogen selenide pools of selenium metabolites. To explore the role of caspases in cancer cell apoptosis induced by selenium, we examined the involvement of these molecules in the death of the DU-145 human prostate carcinoma cells induced by methylseleninic acid (MSeA), a novel penultimate precursor of the putative critical anticancer metabolite CH_3SeH. Sodium selenite, a representative of the genotoxic selenium pool, was used as a reference for comparison. The results show that MSeA-induced apoptosis was accompanied by the activation of multiple caspases (caspase-3, -7, -8, and -9), mitochondrial release of cytochrome c (CC), poly(ADP-ribose) polymerase (PARP) cleavage, and DNA fragmentation. In contrast, selenite-induced apoptotic DNA fragmentation was observed in the absence of these changes, but was associated with the phosphorylation of c-Jun-NH_2-terminal kinase 1/2 and p38 mitogen-activated protein kinase/stress-activated protein kinase 2. A general caspase inhibitor, benzyloxycarbonyl-Val-Ala-Asp-(OMe) fluoromethyl ketone, blocked MSeA-induced cleavage of procaspases and PARP, CC release, and DNA nucleosomal fragmentation, but did not prevent cell detachment. Furthermore, PARP cleavage and caspase activation were confined exclusively to detached cells, indicating that MSeA induction of cell detachment was a prerequisite for caspase activation and apoptosis execution. This process therefore resembled "anoikis," a special mode of apoptosis induction in which adherent cells lose contact with the extracellular matrix. Additional experiments with irreversible caspase inhibitors show that MSeA-induced anoikis involved caspase-3- and -7-mediated PARP cleavage that was initiated by caspase-8 and probably amplified through CC-caspase-9 activation and a feedback activation loop from caspase-3. Taken together, the data support a methyl selenium-specific induction of DU-145 cell apoptosis that involves cell detachment as a prerequisite (anoikis) and is executed principally through caspase-8 activation and its cross-talk with multiple caspases.

INTRODUCTION

The trace element selenium is an essential micronutrient for humans and animals. The current recommended daily allowance is 55 μg for a healthy adult (1). Two human cancer prevention trials have indicated that a supranutritional selenium supplement (*i.e.,* 200 μg daily) might be an effective preventive agent for several major cancers, including those of the prostate, lung, colon (2), and liver (3). The results corroborate findings in various animal models that selenium possesses a potent cancer chemopreventive activity when its intake exceeds the nutritional requirement by $\sim$10-fold (4). The studies in these model systems have provided significant insights on the potential mechanisms of action. It has been shown that a mono-methyl selenium species, possibly methylselenol (CH_3SeH), may be a critical *in vivo* selenium metabolite against chemically induced mammary

carcinogenesis; the cancer preventive efficacy of a given selenium compound may depend on the rate of its metabolic conversion to that active form (4–6). Selenium-enriched garlic, of which selenium-methylselenocysteine constitutes a major selenium component, exerted a lasting protective effect even when provided for as little as 1 month in the early promotion stage of mammary carcinogenesis (7, 8). These findings suggest that a chemopreventive intake of selenium may exert protection against cancer development by inducing the loss of transformed epithelial cells *in vivo*. Because lesion size is governed by the balance between rates of cell proliferation and cell death, the significance of a cell deletion action is further implicated by the lack of a detectable antiproliferative effect of a selenium dose that conferred effective chemoprevention *in vivo* in a chemically induced mammary carcinogenesis model (9).

Regarding the cell deletion action of selenium, our previous work documented distinct proapoptotic effects of different chemical forms (pools) of selenium on mammary tumor epithelial cells *in vitro* (8, 10, 11). Immediate precursors of CH_3SeH, such as selenium-methylselenocyanate and selenium-methylselenocysteine, were shown to induce exclusively apoptosis of mammary tumor epithelial cells without induction of DNA single strand breaks (8, 10). On the other hand, sodium selenite and sodium selenide, which feed into the hydrogen selenide (H_2Se) pool (12), induced DNA single strand breaks (*i.e.,* genotoxic) within a few hours of selenium exposure and subsequent cell death by a composite of acute lysis and apoptosis (10). However, little is known of the execution pathway(s) of methyl selenium-induced cancer cell apoptosis.

Programmed cell death induced by physiological/pathological cues often is characterized by marked changes in cellular morphology, including chromatin condensation, membrane blebbing, nuclear breakdown, and the appearance of membrane-enclosed apoptotic bodies (13). Biochemically, internucleosomal DNA fragmentation and caspase-mediated cleavage of PARP[3] and key cytoskeletal proteins principally underlie these cellular and nuclear changes (14, 15). PARP cleavage essentially inactivates the enzyme by destroying its ability to respond to DNA strand breaks for repair, and it also blocks necrosis resulting from PARP-mediated NAD^+/ATP depletion to ensure an irreversible apoptotic death (16). PARP cleavage has now been recognized as a sensitive marker of caspase-mediated apoptosis.

Caspases are aspartate-specific cysteine proteases, existing as latent intracellular zymogens (14, 15). Once activated by apoptotic signals, they can systematically dismantle the cell by cleaving key cellular and nuclear proteins with defined substrate specificities (14, 15). According to their sequence of action in apoptosis signaling, the more than 14 caspases are organized into apoptotic initiator caspases (caspase-2, -8, -9, and -10), apoptotic executioner caspases (caspase-3, -6, and -7), and cytokine processor caspases (caspase-1, -4, -5, -11, -12, -13, and -14). The initiator caspases appear to have some specificity for dif-

---

[3] The abbreviations used are: PARP, poly(ADP-ribose) polymerase; FADD, Fas-associated death domain (Mort-1); CC, cytochrome c; APAF-1, apoptosis protease activation factor-1; MSeA, methylseleninic acid; zVADfmk, benzyloxycarbonyl-Val-Ala-Asp-(OMe) fluoromethyl ketone; zDEVDfmk, benzyloxycarbonyl-Asp-Glu-Val-Asp-(OMe) fluoromethyl ketone; zIETDfmk, benzyloxycarbonyl-Ile-Glu-Thr-Asp-(OMe) fluoromethyl ketone; zLEHDfmk, benzyloxycarbonyl-Leu-Glu-His-Asp-(OMe) fluoromethyl ketone; PKB, protein kinase B; JNK, c-Jun-NH_2-terminal kinase; SAPK, stress-activated protein kinase; MAPK, mitogen-activated protein kinase; p-NA, *p*-nitroaniline.

3062

ferent types of upstream apoptosis signals as well as preferred downstream substrate procaspases. In fact, two general activation cascades have been described (14–17). The first involves cell death receptor-mediated signaling through caspase-8. Once the receptor is activated, the adapter molecule FADD becomes recruited to the receptor, allowing binding and autocleavage activation of procaspase-8. The active caspase-8 in turn cleaves executioner procaspases (caspase-3, -6, and -7), leading to their activation. The second, termed the "apoptosome" cascade, involves activation of procaspase-9 by CC released from mitochondria. Once in the cytosol, CC binds to APAF-1, which then permits recruitment of procaspase-9, resulting in the oligomerization and autoactivation of procaspase-9. Active caspase-9 then cleaves and activates executioner procaspases. The mitochondrial pathway has been shown to be triggered by diverse chemotherapeutic agents (16, 17). Furthermore, there have been ample examples of cross-talk between these two cascades in many apoptosis models. For example, caspase-8-cleaved BID, a Bcl-2 interacting protein, had been shown to amplify CC release from mitochondria (18, 19). Recent reports have shown a feedback amplification of CC release by downstream effector caspases (20–22). Therefore, depending on the apoptosis signal, the death-receptor/caspase-8 cascade or the CC/APAF-1/caspase-9 cascade can play either a direct initiating or an indirect amplifying role in caspase activation and apoptosis execution.

To explore the role of caspases in cancer cell apoptosis induced by selenium, particularly by CH_3SeH, we examined the involvement of these molecules in the death of the DU-145 human prostate carcinoma cells induced by methylseleninic acid (CH_3SeO_2H; MSeA) in contrast to selenite, used as a reference. MSeA is a novel, penultimate CH_3SeH precursor that is water soluble, nonvolatile, and ideal for cell culture delivery for mechanistic investigations. We chose to use a human prostate carcinoma cell line for this study because the prostate appears to be a sensitive organ site for cancer chemoprevention by selenium in a recent prevention trial (2). Our data show that MSeA-induced nucleosomal DNA fragmentation was accompanied by the activation of multiple caspases (caspase-3, -7, -8, and -9), PARP cleavage, and mitochondrial release of CC, whereas apoptotic DNA fragmentation induced by selenite was observed in the absence of these changes. Furthermore, the data support MSeA induction of cell detachment as a prerequisite for the activation of caspases in an apoptosis execution process resembling "anoikis," a special mode of apoptosis induction in which adherent cells lose contact with the extracellular matrix (23).

MATERIALS AND METHODS

Chemicals and Reagents. Sodium selenite pentahydrate was purchased from J.T. Baker, Inc (Phillipsburg, NJ). MSeA synthesis has been described elsewhere (24), and concentrated stocks were stored in small aliquots at $-80°C$. Intracellularly, MSeA probably reacts with reduced glutathione to generate CH_3SeH. The caspase inhibitors zVADfmk (general), zDEVDfmk (caspase-3 and -7; see Ref. 25 for specificity), zIETDfmk (caspase-8), and zLEHDfmk (caspase-9) were from Enzyme Systems Inc. (Dublin, CA). Reagent kits for CC ELISA and caspase colorimetric activity assays were purchased from R&D Systems (Minneapolis, MN) and used per the manufacturer's instructions. Antibodies for PARP and caspases were purchased from Cell Signaling Technology (apoptosis sampler kit, cat. no. 9915; Beverly, MA) and BD PharMingen (San Diego, CA). Phospho-specific antibodies for AKT/PKB, JNK and p38 MAPK were purchased from New England Biolabs (Beverly, MA).

Cell Culture and Selenium Treatments. DU-145 prostate cancer cells were kindly provided by R. Agarwal (AMC Cancer Research Center), who originally obtained these cells from the American Type Culture Collection. The cells had been passaged ~50 times when we took possession. DU-145 cells were cultured in RPMI 1640 supplemented with 10% fetal bovine serum and 2 mM L-glutamine (no antibiotics). For the DNA fragmentation assay, caspase activity and immunoblot analyses, cells were treated in T75 or T25

flasks. When cells reached 50–70% confluence, the medium was changed, and the cells were treated with selenium or other agents. To standardize selenium exposure, cells were given fresh medium at a volume-to-surface area ratio of 0.2 ml/cm^2 (15 ml for a T75 flask and 5 ml for a T25 flask). Concentrated selenium stock (aqueous solution stored at $-80°C$) was diluted in PBS to 1 mM immediately before use. In experiments in which caspase inhibitors were used, the inhibitors (dissolved in DMSO) and MSeA were mixed into treatment medium first and then fed to cells. DMSO was added to groups that did not receive inhibitors to control for solvent effects. The final concentration of DMSO was $\leq 2 \mu l/ml$ and did not by itself induce adverse cellular responses. Representative morphological responses to selenium exposure were documented with a Polaroid camera at $\times 200$ magnification under a phase-contrast microscope. All experiments were replicated two or more times.

DNA Isolation and Gel Electrophoresis. DNA isolation and gel electrophoresis were as described previously (26). Briefly, after selenium exposure, conditioned medium was collected, and detached cells were recovered by centrifugation at $200 \times g$ for 5 min at room temperature. Adherent cells were lysed and scraped in 1 ml of a buffer containing 10 mM Tris-HCl (pH 8.0), 100 mM EDTA, 0.5% SDS, and 0.5 mg/ml proteinase K and pooled with the detached cells. After digestion at $50°C$ for 3 h, the lysate was extracted twice with phenol-chloroform. Nucleic acids were precipitated with 0.6 volume of isopropanol in the presence of 0.2 M NaCl. The pellet was resuspended in 30 μl of 10 mM Tris-HCl, 1 mM EDTA (pH 7.5); treated with RNase to digest RNA; loaded onto an 1.5% agarose gel containing 0.1 $\mu g/ml$ ethidium bromide; and electrophoresed. Gels were photographed with Polaroid films using UV illumination and digitized with a scanner.

Immunoblot Analyses. After selenium exposure for a defined length of time, detached cells were collected as above by centrifugation. The cell pellet was washed once in ice-cold PBS. Adherent cells were washed twice in PBS, lysed in radioimmunoprecipitation assay buffer [50 mM Tris-HCl (pH 7.4), 150 mM NaCl, 2 mM EDTA, 50 mM NaF, 1% Triton X-100, 1% sodium deoxycholate, 0.1% SDS, 1 mM DTT, 5 mM sodium orthovanadate, 1 mM phenylmethylsulfonyl fluoride, and 38 $\mu g/ml$ aprotinin (added fresh)], and pooled with the detached cell pellet. After sonication, the lysate was centrifuged ($14,000 \times g$ for 20 min at $4°C$), and supernatant was recovered. The protein content was quantified by the Bradford dye-binding assay (Bio-Rad Laboratories, Richmond, CA). Forty (for PARP, AKT, JNK, and p38 MAPK) or 100 μg (for caspases) of total protein were size-separated by electrophoresis on 10, 12, or 15% SDS-polyacrylamide gels, depending on the sizes of target proteins. The proteins were electroblotted onto nitrocellulose membranes and probed using primary antibodies commercially obtained from Cell Signaling Technology, New England Biolabs, or other vendors and detected by enhanced chemiluminescence. In many cases, antibodies from multiple sources for a protein of interest were used to verify specificity of detection. Positive-control samples obtained from the antibody suppliers were used whenever available. The X-ray films were digitized using a transmission scanner, and the signal intensity was quantified using the UN-SCAN-IT gel scanner software (Silk Scientific, Inc., Orem, UT).

Caspase Activity Assays. After selenium treatment of a defined length, the detached cells were harvested by centrifugation at $200 \times g$ for 5 min at room temperature as above, washed once with PBS, and the cell pellets were held on ice. The adherent cells were washed twice with PBS, scraped off in 500 μl of ice-cold lysis buffer provided with R&D Systems caspase assay kits, and pooled with the detached cells. After sonication, the lysate was centrifuged for 20 min at $14,000 \times g$ at $4°C$. The resulting supernatants were analyzed for protein concentration by the Bradford dye-binding assay and stored at $-20°C$ until used for caspase colorimetric enzymatic activity assays per the manufacturer's instruction using 96-well plate. Equal amounts of protein from different treatments were used, and the assays were set up on ice. Absorbance was recorded on a plate reader at 405 nm immediately after the start of the assay and after 10–16 h of incubation at $37°C$. The net increase of absorbance was indicative of enzyme activity.

CC Assay. Mitochondria-free cytosol was prepared according to a method described for prostate cancer cells (27). Briefly, after selenium treatment of a defined length, the detached floaters were harvested by centrifugation at $200 \times g$ for 5 min at room temperature as above, washed once with PBS, and the cell pellets were held on ice. The adherent cells were washed twice with PBS, scraped off in 500–700 μl of ice-cold hypotonic buffer [20 mM HEPES-KOH (pH 7.4), 10 mM KCl, 1.5 mM $MgCl_2$, 1 mM sodium EDTA, 1 mM

3063

A. Phase contrast morphology
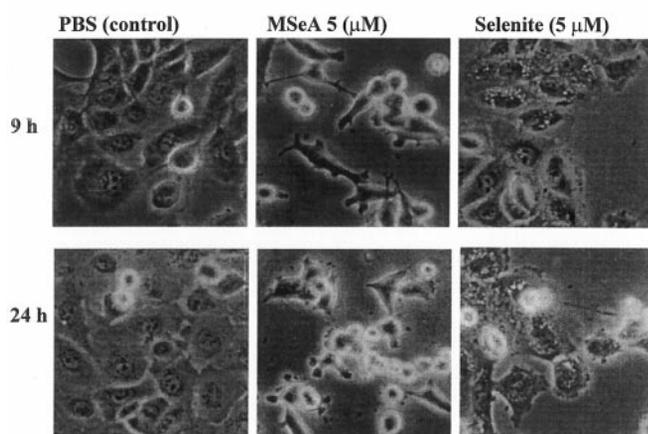
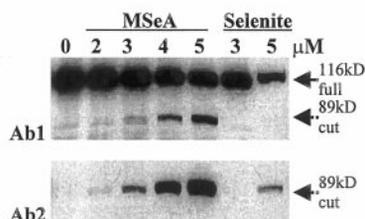**B. DNA fragmentation at 24 h**
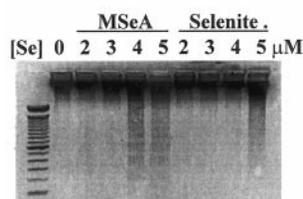
C. PARP Cleavage at 24 h

Fig. 1. *A,* phase contrast photomicrographs depicting representative morphological responses of DU-145 prostate cancer cells at 9 and 24 h of exposure to 5 μM MSeA or selenite. Note profound cell retraction and rounding at 9 h and detached or loosely adhered rounded cells at 24 h for MSeA-treated cells. For selenite-exposed cells, note prominent cytosolic vacuoles in adherent cells at 9 h and vacuolated adherent cells and floaters (out of focus) at 24 h. Magnification, ×200. *B*, agarose gel (1.5%) electrophoretic detection of nucleosomal DNA fragmentation at 24 h of exposure to increasing concentrations of MSeA or selenite. The *leftmost lane* was loaded with 100-bp DNA size markers. Inverted image was used to better show fragmented DNA. *C*, immunoblot detection of PARP cleavage at 24 h of exposure to increasing concentrations of MSeA or selenite. Antibody 1 (*Ab1*) detected both the full-length (116 kDa) and cleavage product (89 kDa) of PARP. The increased sensitivity of detection by *Ab2* in the *bottom panel* was attributable to the use of an antibody that specifically recognized only the cleaved PARP (cat. no. 9915; Cell Signaling Technology). Adherent cells and detached floaters were combined for cell lysate preparations for these analyses.

sodium EGTA, 1 mM DTT, 250 mM sucrose, and protease inhibitors], and pooled with floaters. After incubation on ice for 20 min, cells were further disrupted by Dounce homogenization for 50 strokes. Nuclei and cellular debris were removed by centrifugation at 1000 × *g* for 10 min at 4°C. Supernatants were further centrifuged for 20 min at 14,000 × *g* at 4°C to pellet mitochondria. The resulting supernatants were analyzed for protein concentration by Bradford dye binding and stored at −80°C until analyzed for CC content using an ELISA kit from R&D Systems. Equal amounts of protein from different treatments were used for these assays.

RESULTS

Morphological Responses and DNA Nucleosomal Fragmentation. Exposure of DU-145 cells in log-phase monolayer culture to 5 μM MSeA led to cell retraction (elongated rod shapes) and rounding by 9 h and subsequent detachment of individual cells from the culture vessels (Fig. 1*A*). Some, but not all, detached cells (floaters) displayed the grape-like fragmented morphology typical of apoptotic bodies under a phase-contrast microscope. In contrast, exposure to sodium selenite led to the appearance of prominent cytoplasmic vacuoles by 9 h and detached floaters later (Fig. 1*A*). Despite the different morphological responses elicited by the two forms of selenium, both MSeA- and selenite-treated cells displayed DNA nucleosomal fragmentation typical of apoptotic cell death at 24 h of exposure (Fig. 1*B*).

PARP Cleavage Was Detected Mainly in MSeA-exposed Cells. In dose-response experiments, PARP cleavage was detected in MSeA-treated cells after 24-h exposure at as low as 3 μM and increased in a dose-dependent manner (Fig. 1*C*). On the other hand, PARP cleavage was minimal in cells exposed to 5 μM selenite (Fig. 1*C*) that had undergone a comparable extent of DNA nucleosomal fragmentation (Fig. 1*B*). Instead, the level of full-length PARP expression decreased in selenite-exposed apoptotic cells. These results indicate that PARP cleavage was involved in apoptosis execution induced by MSeA, but was minimally, if at all, involved in apoptosis induced by selenite within the time frame of the study.

Multiple Caspase Activities and Mitochondrial Release of CC Were Detected in MSeA-exposed, but not Selenite-exposed, Cells. To define which caspases were involved in PARP cleavage during apoptosis induced by MSeA, we analyzed the enzymatic activities of DU-145 cell lysates against tetrapeptide substrates DEVDp-NA (for caspases-3 and caspase-7), IETDp-NA (for caspase-8) and LE-HDp-NA (for caspase-9) after 24-h exposure to 5 μM selenium as either MSeA or selenite (Fig. 2, *A–C*). The relative hydrolytic activities toward the respective substrates were 5.3-, 1.7-, and 2.1-fold in MSeA-treated cells compared with untreated control cells, whereas no changes in the activities of these enzymes were detected in the
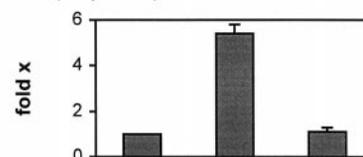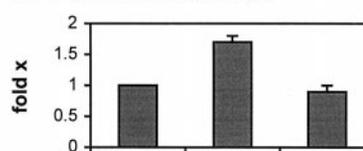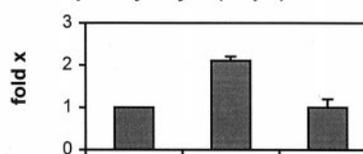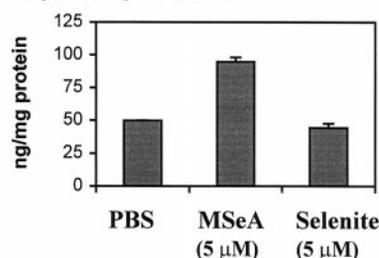

Fig. 2. *A–C*, enzymatic activities of cell lysates toward tetrapeptide caspase substrates in DU-145 prostate cancer cells at 24 h of exposure to 5 μM MSeA or selenite. The chromogenic substrates were DEVD-pNA (caspase-3-like and caspase-7; *A*), IETD-pNA (caspase-8; *B*), and LEHD-pNA (caspase-9; *C*). The caspase activity was expressed as fold relative to untreated controls and represented mean and SD (*bars*) of three independent experiments done on different occasions. *D*, CC content in postmitochondrial cytosol preparations of DU-145 prostate cancer cells at 24 h of exposure to 5 μM MSeA or selenite measured using a CC ELISA. Adherent cells and floaters were combined for the analyses of caspases and CC. Protein contents of the cell lysates were measured to equalize input of protein from different groups for each assay.

3064

A

- MSeA Sel 5μM

DNA

Total PARP — 116kD full (solid arrow), 89kD cleaved (dashed arrow)

— 55/50kD full (solid arrow), 43/41kD intermediates (dashed arrow)

Total Caspase-8 — 18kD (dashed arrow)

Cleaved Casp-9 — 37kD (dashed arrow)

Cleaved Casp-7 — 20kD (dashed arrow)

— 32kD full (solid arrow), Intermediates? (dashed arrow)

Cleaved Casp-3

B Protein kinases

Phospho-AKT — 60kD (solid arrow)

Total AKT — 60kD (solid arrow)

Phospho-JNK — pJNK1 54kD (solid arrow), pJNK2 46kD (solid arrow)

Phospho-p38MAPK — ~40kD (solid arrow)

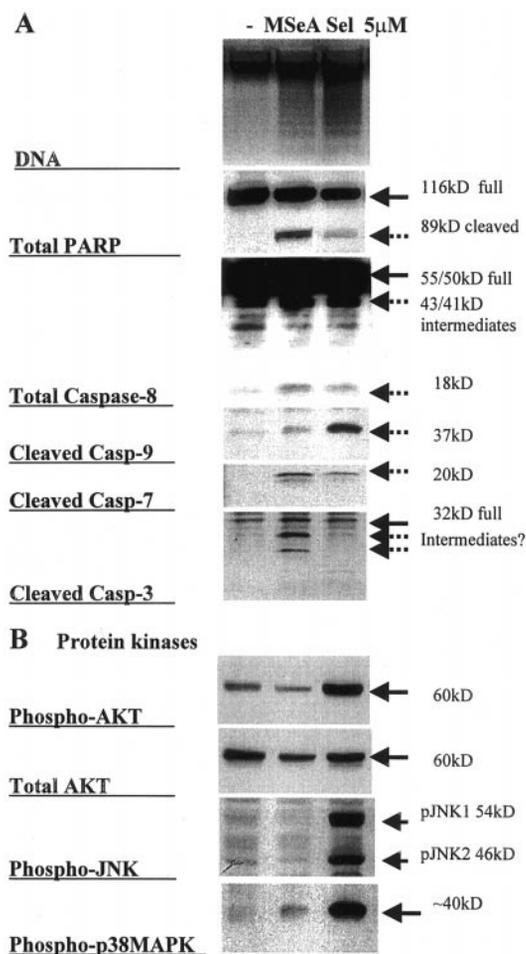Fig. 3. *A*, immunoblot analyses of the cleavage patterns of selected caspases in DU-145 prostate cancer cells at 26 h of exposure to 5 μM selenium as MSeA or selenite (*Sel*). *Solid arrows* indicate full-length proteins. *Dashed arrows* indicate cleavage intermediates and final products. ? indicates that intermediates have not been identified. *B*, phosphorylation status of selected protein kinases involved in cell survival and cellular stress and apoptosis signaling in DU-145 prostate cancer cells at 24 h of exposure to 5 μM selenium as MSeA or selenite. Adherent cells and floaters were combined for cell lysate preparations for immunoblot analyses.

selenite-treated cells. The cytosolic CC level was increased 2-fold in the MSeA-treated cells, but not in selenite-treated cells (Fig. 2*D*). These results indicate that CC release might be involved in some aspect of caspase activation in MSeA-induced apoptosis.

By immunoblot detection, cleavage of procaspase-8, -9, -3, and -7 was detected in MSeA-treated cells at 26 h of exposure, corresponding to significant PARP cleavage and DNA fragmentation (Fig. 3*A*). On the other hand, selenite-exposed cells did not cleave procaspase-3, slightly increased procaspase-7 cleavage, and minimally cleaved PARP despite pronounced DNA nucleosomal fragmentation (Fig. 3*A*). Paradoxically, the extent of procaspase-9 cleavage in the selenite-treated cells was much greater than in MSeA-treated cells (Fig. 3*A*), although caspase-9 activity was not detected in the selenite-treated cells (Fig. 2*C*). Similarly, selenite-exposed cells underwent increased cleavage of procaspase-8 compared with untreated control cells, but failed to hydrolyze the IETDp-NA substrate in the caspase-8 enzyme assay.

The discrepancy between procaspase-9 cleavage (suggesting activation; Fig. 3*A*) and the lack of measurable hydrolysis of LEHDp-NA (Fig. 2*C*) in selenite-exposed cells might be in part attributable to increased phosphorylation (suggesting activation) of AKT/PKB (Fig. 3*B*), a survival enzyme (28) that has been shown to inhibit apoptosis

at least in part through an inactivation of caspase-9 (29) and the proapoptotic BAD protein (30, 31) by phosphorylation. The selenite-exposed cells, but not those treated with MSeA, also had a significant induction of the phosphorylation of JNK1 (p54), JNK2 (p46), and p38 MAPK/SAPK2 (Fig. 3*B*), two protein kinase pathways that have been linked to stress responses and apoptosis (32). These results suggest potential alternative pathways that might contribute to selenite-induced apoptosis signaling and execution independent of caspases and PARP cleavage.

Temporal Relationship of Caspase Activation and PARP Cleavage in MSeA-exposed Cells. To further define the involvement of caspase in MSeA-induced apoptosis, we analyzed the kinetic patterns of procaspase cleavage in time course experiments (Fig. 4). In an acute exposure setting (experiment 1), the appearance of procaspase-8 cleavage intermediates of 43 or 41 kDa was observed at 6 h, whereas the final cleavage products of procaspase-8, -9, and -7 were detectable by 10 h of exposure when PARP cleavage became apparent. The activation of these three enzymes preceded induction of the expression of what appeared to be cleavage intermediate(s) of procaspase-3 by at least 2 h. In experiment 2, the levels of cleaved caspase-8 and -9 peaked at 16 h, whereas those for caspase-3 and -7 peaked at 20 h. These cleavage patterns suggest that the initial PARP cleavage before caspase-3 activation was likely attributable to cleaved caspase-7 or -9 and that, once activated, caspase-3 might further amplify PARP cleavage.

Measurement of enzyme activity indicated that hydrolysis of IETDp-NA (caspase-8 activity) increased significantly at 12 h of MSeA exposure and peaked at 16 h, whereas hydrolysis of DEVDp-NA (caspase-3 and -7 activity) increased with the same time frame, but peaked at 20 h (Fig. 5). The hydrolysis of LEHDp-NA (caspase-9 activity) also peaked at 20 h (Fig. 5). Together, the cleavage patterns and activity measurements suggest that the activation of caspase-8 was mostly an upstream event for caspase-mediated PARP cleavage during MSeA-induced apoptosis.

A General Caspase Inhibitor Abolished MSeA-induced PARP Cleavage, CC Release, and DNA Fragmentation. Cotreatment of DU-145 cells with zVADfmk (80 μM) blocked, as expected, MSeA-induced cleavage of procaspase-8, -9, -3, and -7 completely at 20 h of exposure (Fig. 6*A*). This general caspase inhibitor also completely blocked PARP cleavage and DNA fragmentation (Fig. 6*A*) and mitochondrial CC release (Fig. 6*B*). These results indicate that these three events are caspase dependent and that the CC/caspase-9 activation cascade might be a secondary amplification, rather than an initiating, pathway in MSeA-induced apoptosis execution.

Contrary to its inhibitory efficacy on these apoptosis-execution events, zVADfmk did not block cell retraction and rounding, nor did it decrease the number of cells that subsequently detached to become floaters by 20 h (Fig. 6*C*). Cleavage of PARP and procaspase-3 and -7 was detected exclusively in the MSeA-induced floaters, and was not detectable in the adherent cells (Fig. 6*C*). The inhibitor blocked the cleavage of procaspase-3 and -7 and PARP in the MSeA-induced floaters (Fig. 6*C*). These observations indicate that MSeA-induced cell detachment is a prerequisite for caspase activation and PARP cleavage. This mode of apoptosis induction closely resembled anoikis, in which adherent cells undergo apoptosis after becoming detached from the extracellular matrix (23).

Effects of Specific Caspase Inhibitors on MSeA-induced PARP Cleavage and DNA Fragmentation. To delineate the relative contributions of the various caspases, especially with reference to the two activation cascades described in the "Introduction" (14, 15) for MSeA-induced PARP cleavage, we next examined the impacts of irreversible caspase inhibitors zIETDfmk (for caspase-8), zLEHDfmk (for caspase-9), zDEVDfmk (for caspase-3 and, at higher level, for
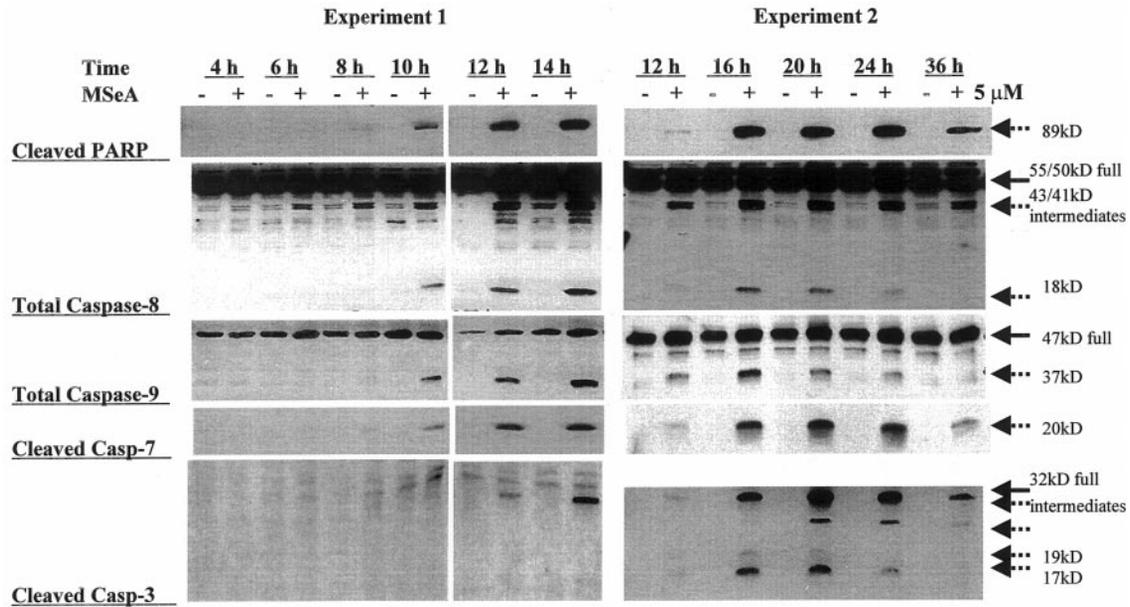
3065

Fig. 4. Immunoblot analyses of the time course of MSeA-induced cleavage of PARP and selected caspases in DU-145 prostate cancer cells exposed to 5 μM MSeA. Adherent cells and floaters were combined for cell lysate preparations for these immunoblot analyses. The experiments were conducted several weeks apart, which might account for the slight difference in the time of onset of caspase activation and PARP cleavage between them. *Solid arrows* indicate full-length proteins; *dashed arrows* indicate possible cleavage intermediates and final products.

caspase-7; Ref. (25) and zVADfmk (for all caspases) at a concentration of 40 μM for each inhibitor. As shown in Fig. 7A, at 40 μM the general caspase inhibitor zVADfmk completely blocked MSeA-induced PARP cleavage, which is in excellent agreement with the data presented in Fig. 6 for 80 μM inhibitor. The caspase-8 inhibitor zIETDfmk decreased PARP cleavage by 90%, and the caspase-9 inhibitor zLEHDfmk decreased PARP cleavage by 40%. When the two inhibitors were used together, the effect was the same as for the caspase-8 inhibitor alone, indicating that caspase-9 might be a downstream component of the caspase-8 activation cascade rather than as an independent pathway.

The effects of these inhibitors on the caspase cleavage patterns and PARP cleavage provided further support for this scenario. As shown in Fig. 7B, the caspase-8 inhibitor zIETDfmk decreased the cleavage of procaspase-9 by 90% and completely blocked the generation of the cleaved caspase-7 (20 kDa) and caspase-3 (17 kDa). The caspase-9 inhibitor zLEHDfmk decreased the extent of active caspase-3 (17 kDa product) by 60% and active caspase-7 by 70%, whereas it had little effect on the accumulation of the cleaved caspase-9 itself. Blockage of the caspase-8 activity decreased the extent of MSeA-induced PARP cleavage by 90%, and the caspase-9 inhibitor decreased PARP cleavage by 60% in this experiment, in good agreement with the previous experiment.

The caspase-3-like inhibitor zDEVDfmk blocked MSeA-induced PARP cleavage by ~97%, establishing caspase-3 as a major player in PARP cleavage (Fig. 7B) with minor contribution from caspase-7 to this activity. Surprisingly, this inhibitor produced nearly complete inhibition not only of caspase-3 cleavage, but also of caspase-9 cleavage. These results, coupled with the delayed activation of caspase-3 in the time course experiments (Fig. 4), suggest a possible feedback loop from caspase-3 to caspase-9. zDEVDfmk significantly reduced (~80%) but did not completely block procaspase-7 cleavage, which might be attributable to the initial caspase-8 and -9 activities leading to procaspase-7 cleavage before the feedback loop from caspase-3 was established. On the basis of these cleavage patterns and the fact that zVADfmk blocked CC release from mitochondria (Fig.
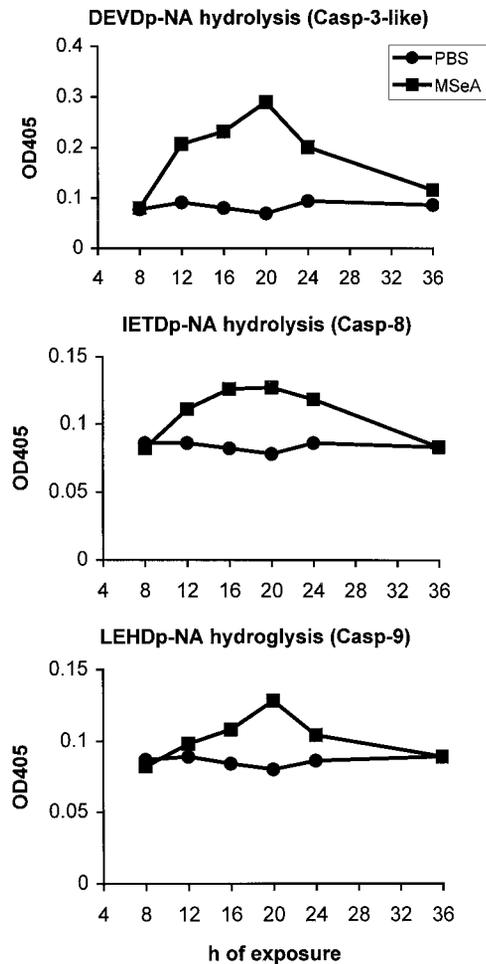
Fig. 5. Time course of caspase substrate hydrolysis activities in DU-145 prostate cancer cells exposed to 5 μM MSeA. Adherent and detached cells were pooled for lysate preparation for the enzyme assays. The chromogenic substrates used were DEVDp-NA (for caspase-3 and 7), IETDp-NA (for caspase-8), and LEHDp-NA (for caspase-9), respectively. High background absorbance (*OD*) in controls was attributable to protein precipitation over the course of a ≥10-h incubation. Each *point* represents the mean of duplicate flasks, each with triplicate measurements.

3066

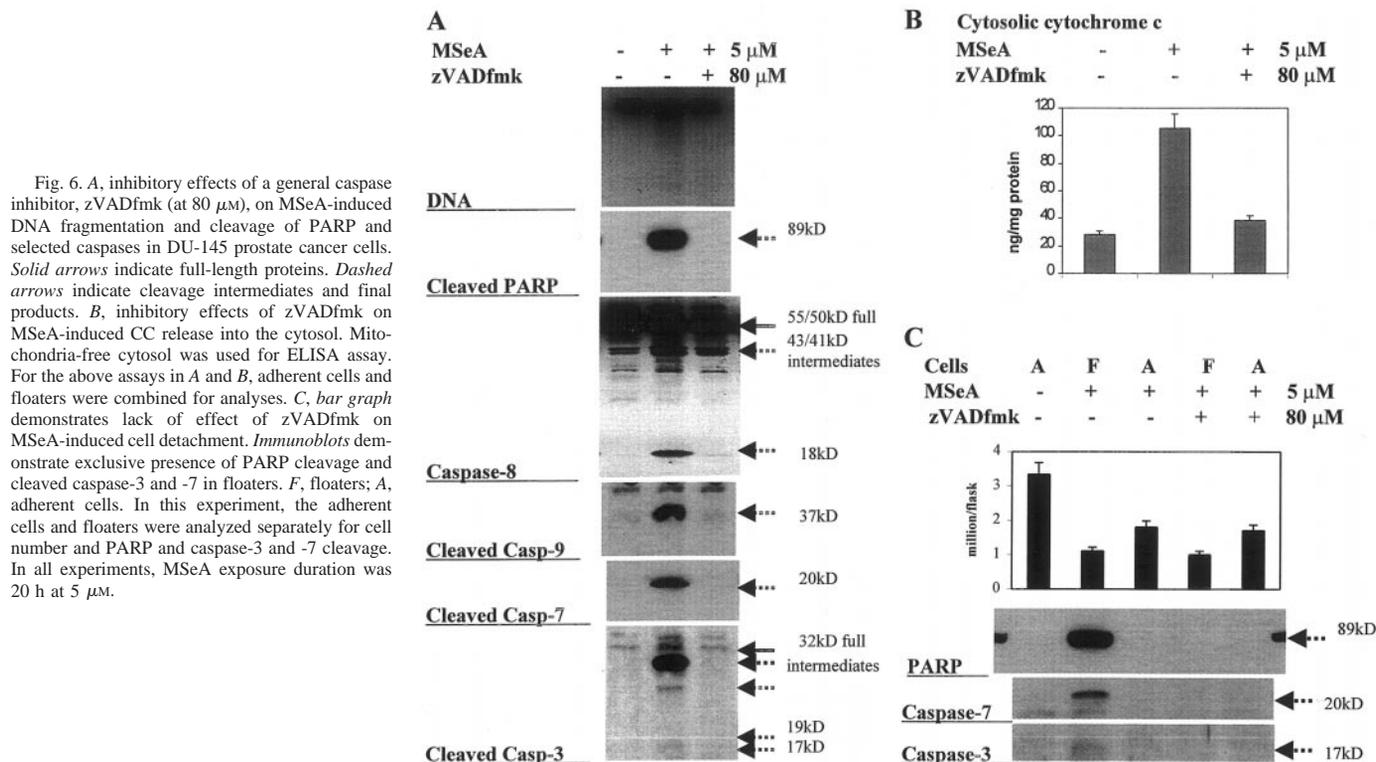Fig. 6. *A*, inhibitory effects of a general caspase inhibitor, zVADfmk (at 80 μM), on MSeA-induced DNA fragmentation and cleavage of PARP and selected caspases in DU-145 prostate cancer cells. *Solid arrows* indicate full-length proteins. *Dashed arrows* indicate cleavage intermediates and final products. *B*, inhibitory effects of zVADfmk on MSeA-induced CC release into the cytosol. Mitochondria-free cytosol was used for ELISA assay. For the above assays in *A* and *B*, adherent cells and floaters were combined for analyses. *C*, *bar graph* demonstrates lack of effect of zVADfmk on MSeA-induced cell detachment. *Immunoblots* demonstrate exclusive presence of PARP cleavage and cleaved caspase-3 and -7 in floaters. *F*, floaters; *A*, adherent cells. In this experiment, the adherent cells and floaters were analyzed separately for cell number and PARP and caspase-3 and -7 cleavage. In all experiments, MSeA exposure duration was 20 h at 5 μM.

6*B*), we propose a putative scheme of caspase-3 feedback activation of caspase-9 through a mitochondria/CC release mechanism (see Fig. 8).

In addition, the various inhibitors did not block the conversion of procaspase-8 to the 43/41 kDa intermediate forms, but appeared to inhibit the generation or maturation of the 18-kDa active caspase-8 form as indicated by the retarded migration of the expected band (Fig. 7*B*). These observations suggest a possible feedback loop from the downstream caspases, most likely caspase-3, to caspase-8 for the full activation/processing of caspase-8 in MSeA-exposed DU-145 cells (see Fig. 8).

Despite the effective blockage of PARP cleavage by zDEVDfmk or zIETDfmk, DNA fragmentation was detected, albeit at a reduced extent compared with MSeA exposure alone (Fig. 7*B*). These results, together with the complete blockage of DNA fragmentation (Fig. 6*A*) and PARP cleavage (Figs. 6*A* and 7*A*) by the general caspase inhibitor zVADfmk, indicate the likelihood that additional caspases contribute to DNA fragmentation activity and PARP cleavage induced by MSeA exposure (see Fig. 8).

DISCUSSION

Two Selenium Metabolite Pools Induce Prostate Cancer Cell Apoptosis Execution by Distinct Mechanisms. The data presented above document for the first time, to our knowledge, the involvement of PARP cleavage (Fig. 1) and the activation of multiple caspases (Figs. 2 and 3) during apoptosis execution induced by a mono-methyl selenium compound, MSeA. The data also ruled out caspase activation during the same time frame for apoptosis execution induced by selenite, which has been shown by us and others to be genotoxic (8, 10, 11, 26). Instead, apoptotic DNA fragmentation in selenite-exposed cells was associated with the phosphorylation of JNK1/2 and p38 MAPK/SAPK2, whereas these two stress- and apoptosis-signaling kinases (32) were not phosphorylated in the MSeA-treated cells (Fig. 3*B*). Furthermore, selenite exposure increased the phosphorylation of AKT/PKB (Fig. 3*B*), a protein kinase known to mediate cell survival

in many cell types (28). The activation of AKT provides one potential explanation for the inactivation of caspase-9 in selenite-treated cells (Fig. 2 *versus* Fig. 3) through AKT-mediated caspase-9 phosphorylation (29). A recent report has shown that nanomolar concentrations of selenite inhibited caspase-3 activity by a redox mechanism both in the test tube and in cell culture (33). It is therefore possible that selenite might have also inhibited the activities of caspase-8 and -9 as well as caspase-3 in our study (Fig. 2, *A–C*) through a redox modification of the critical cysteine residual in the active center of each caspase. Taken together, these data with the two selenium compounds clearly demonstrate that distinct modes of apoptosis signaling and execution were induced in DU-145 cells by the two metabolite pools, as diagramed schematically in Fig. 8. These results agree with and extend our earlier findings of the differential biochemical and cellular actions of these two selenium pools with mammary cancer cells (10, 11).

Caspases as Essential Executors of MSeA-induced Apoptosis (Anoikis). Pertaining to the role of caspases in MSeA-induced PARP cleavage and apoptosis execution, the general caspase inhibitor zVADfmk completely blocked MSeA-induced CC release, PARP cleavage, and DNA fragmentation, establishing caspase activation as an essential and necessary upstream mediating event of these apoptotic processes (Fig. 6, *A* and *B*). However, it did not prevent MSeA-induced cell detachment (Fig. 6*C*), and caspase-3 and-7 activation and PARP cleavage were detected exclusively in the MSeA-induced floaters, but not in the MSeA-exposed adherent cells (Fig. 6*C*). These results support MSeA-induced cell detachment as a prerequisite for caspase activation. This mode of cell death induction closely resembles detachment-induced anoikis (23).

As mentioned in the "Introduction," two caspase-activation cascades, *i.e.,* the death receptor/caspase-8 pathway and the CC/APAF-1/caspase-9 apoptosome pathway, have been demonstrated for activation of downstream executioner caspases in numerous apoptosis models (14–17). As far as caspase cascades involved in anoikis are
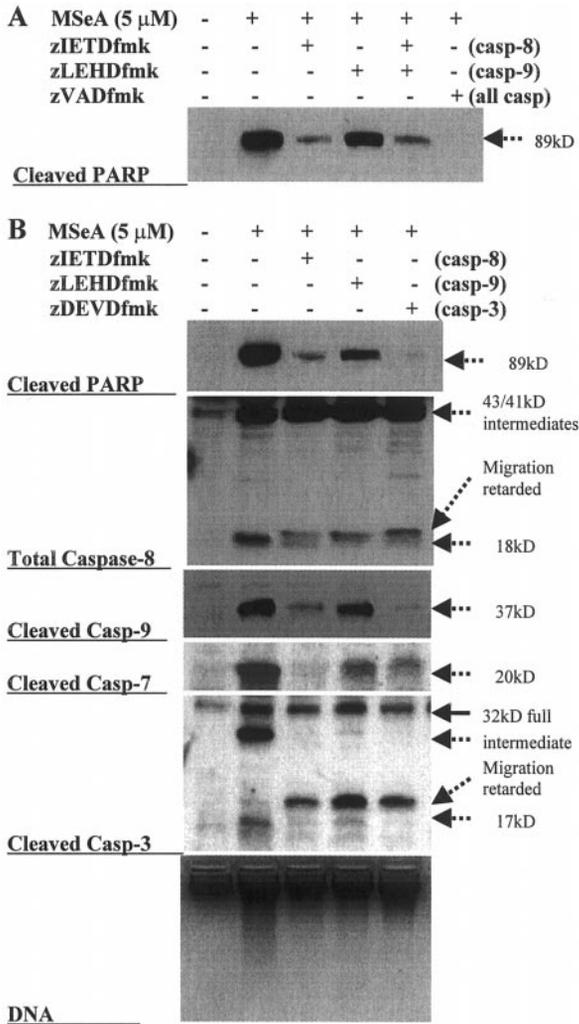
A MSeA (5 μM) ... zIETDfmk (casp-8) ... zLEHDfmk (casp-9) ... zVADfmk (all casp)

Cleaved PARP — 89kD

B MSeA (5 μM) ... zIETDfmk (casp-8) ... zLEHDfmk (casp-9) ... zDEVDfmk (casp-3)

Cleaved PARP — 89kD

43/41kD intermediates
Migration retarded

Total Caspase-8 — 18kD

Cleaved Casp-9 — 37kD

Cleaved Casp-7 — 20kD

32kD full
intermediate
Migration retarded

Cleaved Casp-3 — 17kD

DNA

Fig. 7. *A*, effects of a general caspase inhibitor (*zVADfmk*) and an inhibitor of caspase-8 (*zIETDfmk*) or caspase-9 (*zLEHDfmk*), individually or combined, on MSeA-induced PARP cleavage in DU-145 cells at 20 h of exposure. *B*, effects of an inhibitor of caspase-8, caspase-9 or caspase-3 (*zDEVDfmk*) on MSeA-induced cleavage of PARP and selected caspases and DNA fragmentation in DU-145 cells at 20 h of exposure. In both experiments, each inhibitor was used at a final concentration of 40 μM. Both adherent cells and floaters were combined for these analyses. *Solid arrows* indicate expected full-length proteins. *Dashed arrows* indicate cleavage intermediates and final products. *Diagonal arrows* indicate unidentified cleavage intermediates with altered migration patterns.

activity for PARP cleavage than either caspase-7 or -9 (25), the delayed cleavage of caspase-3 subsequent to the activation of caspase-8, -9, and -7 might account for the accelerated PARP cleavage once apoptosis execution has initiated.

Using irreversible inhibitors for selected caspases, we attempted to further delineate the paths of caspase activation and their relationship to PARP cleavage and DNA fragmentation induced by MSeA (Fig. 7). Several lines of evidence support the scenario that the CC/caspase-9 cascade may be an integral component, rather than an independent pathway, of the death receptor/caspase-8 activation cascade(s). First, as shown in Fig. 7A, the caspase-8 inhibitor blocked PARP cleavage to the same extent as both caspase-8 and caspase-9 inhibitors used together. As shown in Fig. 7B, the caspase-8 inhibitor almost completely blocked procaspase-9 cleavage as well as cleavage of procaspase-7 and -3. The caspase-9 inhibitor, on the other hand, decreased but did not completely block the extent of cleavage of procaspase-3 (to the 17-kDa active product) or procaspase-7, although it had little effect on the accumulation of the cleaved caspase-9 itself. The latter outcome would be predicted from a serial upstream-downstream, rather than a parallel, relationship between caspase-8 and -9. How caspase-8 mediates activation of caspase-9, whether via a direct cleavage effect or BID-induced CC release/caspase-9 activation (17, 18), remains to be determined.

zDEVDfmk (a more potent inhibitor for caspase-3 than for caspase-7; Ref. 25) almost completely blocked PARP cleavage (Fig. 7B), which is consistent with the primary effector role of caspase-3 in executing PARP cleavage as documented in many other model sys-
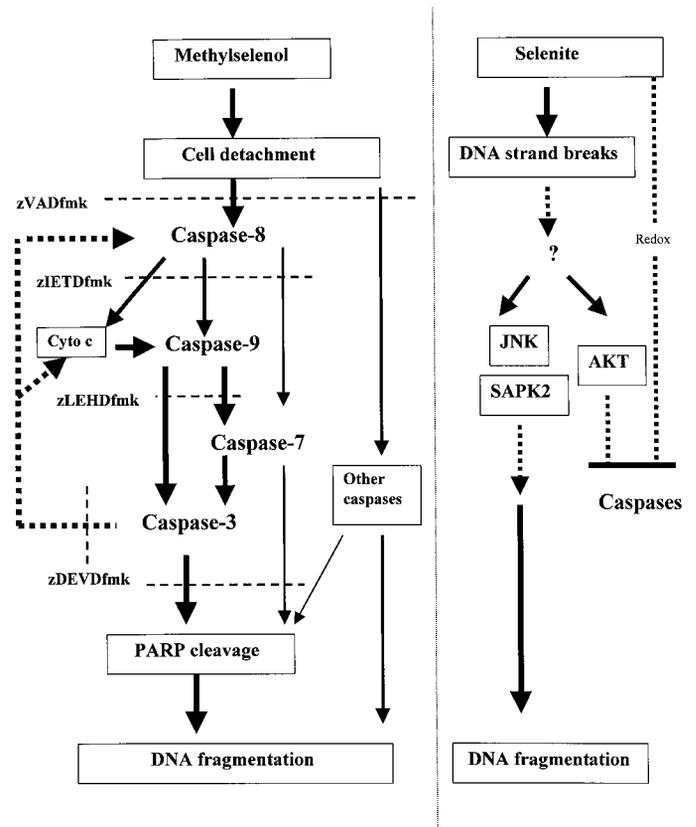
concerned, it has been shown that detachment-induced apoptosis requires death receptor-related and death domain-containing proteins (34) and that apoptosis is blocked by a dominant-negative form of FADD (35). In these studies, detachment induced strong activation of caspase-8 and -3 (34, 35). In addition, recent reports have shown a caspase-dependent CC release from mitochondria during anoikis (36). These findings support the primary role of the death receptor/caspase-8 pathway for anoikis execution with the CC/caspase-9 cascade as a secondary amplification pathway. This generalization appears to fit the patterns of caspase activation induced by MSeA in DU-145 cells as discussed next.

Caspase-8 Is Functionally Upstream of Other Caspases with Potential Feedback Loop(s) in MSeA-induced Anoikis. The temporal sequence of MSeA-induced caspase cleavage patterns (Fig. 4) indicated that the activation of caspase-8 (*e.g.,* occurrence of p43/p41 cleavage intermediates) preceded caspase-9 and -7, all of which occurred prior to activation of caspase-3. The activity measurements were consistent with the temporal kinetic patterns of activation observed above (Fig. 5). Because caspase-3 has much higher specific

Fig. 8. Proposed pathways of MSeA-induced caspase activation and relationships to mitochondria release of CC (*cyto c*), PARP cleavage, and DNA nucleosomal fragmentation during apoptosis execution in DU-145 prostate cancer cells. *Solid arrows* indicate probable events. *Dashed arrows* indicate likely feedback loops from caspase-3 to upstream initiator caspases. *Thin dashed lines* indicate steps where caspase inhibitors used in this study exert their effects. Selenite-induced changes are outlined on the *right* for comparison. The gentotoxic activity of selenite (DNA single strand breaks) was based on our earlier results in leukemia and mammary cancer cell lines (8, 10, 26).

tems (14–17). zDEVDfmk not only blocked the activation of caspase-3, but also significantly decreased cleavage of procaspase-9, indicating that a feedback loop might be involved in the full activation of the caspase-9 cascade (Fig. 7*B*). Recently, caspase-3 activation has been shown to amplify CC release from the mitochondria, via cleavage of either BID or Bcl-2 (20–22). The fact that CC release from mitochondria in MSeA-exposed cells was caspase dependent (Figs. 2 and 6) suggests that the CC/APAF-1/caspase-9 cascade may also be a part of the feedback amplification loop for overall MSeA-induced PARP cleavage (Fig. 8). In addition to the feedback loop from caspase-3 to caspase-9, our data appear to also indicate a feedback loop from caspase-3 to caspase-8 (Fig. 8). The various inhibitors, including zDEVDfmk for caspase-3, did not block the conversion of pro-caspase-8 to the 43/41 kDa intermediate forms, but appeared to inhibit the generation or maturation of the 18-kDa active form of caspase-8 as indicated by the retardation of migration (Fig. 7*B*). Studies are in progress to test these hypotheses.

Additional Caspases Might Contribute to MSeA-induced DNA Fragmentation Activity. Although the inhibition data support the prominent role of caspase-8 → caspase-9, -7 → caspase-3 for PARP cleavage, these caspases do not fully account for DNA fragmentation as a result of exposure to MSeA (Fig. 7*B*). These results, when considered together with the complete blockage of DNA fragmentation by zVADfmk (Fig. 6), suggest that additional caspases may contribute to the DNA fragmentation activity in MSeA-exposed DU-145 cells (Fig. 8).

Relevance of Anoikis Induction by Methyl Selenium in Cancer Chemoprevention. The remarkable efficacy of MSeA in inducing DU-145 cancer cell apoptosis as judged by PARP cleavage (~3 μM; Fig. 1*C*) is noteworthy. As reference values, the mean plasma selenium concentration of subjects without selenium supplementation in the recent human trial was ~1.5 μM (2). Selenium supplementation (200 μg/day as selenized yeast) that was associated with a >50% reduction in the risk for prostate, colon, and lung cancers brought the mean selenium level to ~2.5 μM (2). DU-145 prostate cancer cells, originally derived from an aggressive metastatic carcinoma, are independent of androgen for growth, capable of anchorage-independent growth (*i.e.,* resistant to anoikis), and have extended survivability upon trophic factor withdrawal (37). Therefore, the apoptosis (anoikis) sensitivity of such malignant cells to MSeA would be expected to be much lower than that of transformed prostate epithelial cells in early lesions, which represent the likely targets of chemoprevention by selenium. Although the work reported here focused on induction of anoikis of this aggressive metastatic prostate cancer cell line by MSeA treatment, we speculate that the anoikis mechanism may apply to prostate epithelial cells in early lesions in a pharmacological as well as a chemoprevention context. In other words, achievable serum levels of MSeA might be enough to induce anoikis of transformed prostate epithelial cells in early lesions. Further work is needed to establish the relevance of induction of anoikis by methyl selenium for the chemoprevention of prostate carcinogenesis.

In summary, the data show that MSeA-induced DU-145 cell detachment is a prerequisite for caspase activation and PARP cleavage in an apoptosis execution pathway that is principally initiated by caspase-8 → caspase-9, -7 → caspase-3 and is likely amplified by feedback loop(s) from caspase-3. Many mechanistic questions remain. For example, is integrin-signaling inhibition involved in MSeA induction of cell detachment and caspase activation? Are death receptor molecules and their adapters, such as FADD, involved in the initial stage of caspase-8 activation? Does the AKT/PKB survival pathway, whose phosphorylation was decreased at 24 h of exposure to MSeA, play a role in MSeA-anoikis signaling and execution? Are the Bcl-2 family of anti- and pro-apoptosis proteins, such as Bid and BAD,

involved in MSeA-induced anoikis? Answers to these questions will help to elucidate how methyl selenium triggers the signaling and execution of cancer cell anoikis.

REFERENCES

1. Institute of Medicine, Food, and Nutrition Board. Dietary Reference Intakes. Vitamin C, Vitamin E, Selenium, and Carotenoids. Washington, DC: National Academy Press, 2000.
2. Clark, L. C., Combs, G. F., Jr., Turnbull, B. W., Slate, E. H., Chalker, D. K., Chow, J., Davis, L. S., Glover, R. A., Graham, G. F., Gross, E. G., *et al.* Effects of selenium supplementation for cancer prevention in patients with carcinoma of the skin. A randomized controlled trial. Nutritional Prevention of Cancer Study Group. JAMA, *276:* 1957–1963, 1996.
3. Yu, S. Y., Zhu, Y. J., and Li, W. G. Protective role of selenium against hepatitis B virus and primary liver cancer in Qidong. Biol. Trace Elem. Res., *56:* 117–124, 1997.
4. Ip, C. Lessons from basic research in selenium and cancer prevention. J. Nutr., *128:* 1845–1854, 1998.
5. Ip, C., and Ganther, H. E. Activity of methylated forms of selenium in cancer prevention. Cancer Res., *50:* 1206–1211, 1990.
6. Ip, C., Hayes, C., Budnick, R. M., and Ganther, H. E. Chemical form of selenium, critical metabolites, and cancer prevention. Cancer Res., *51:* 595–600, 1991.
7. Ip, C., Lisk, D. J., and Thompson, H. J. Selenium-enriched garlic inhibits the early stage but not the late stage of mammary carcinogenesis. Carcinogenesis (Lond.), *17:* 1979–1982, 1996.
8. Lu, J., Pei, H., Ip, C., Lisk, D., Ganther, H., and Thompson, H. J. Effect of an aqueous extract of selenium enriched garlic on *in vitro* markers and *in vivo* efficacy in cancer prevention. Carcinogenesis (Lond.), *17:* 1903–1907, 1996.
9. Ip, C., Thompson, H. J., and Ganther, H. E. Selenium modulation of cell proliferation and cell cycle biomarkers in normal and premalignant cells of the rat mammary gland. Cancer Epidemiol. Biomark. Prev., *9:* 49–54, 2000.
10. Lu, J., Jiang, C., Kaeck, M., Ganther, H., Vadhanavikit, S., Ip, C., and Thompson, H. Dissociation of the genotoxic and growth inhibitory effects of selenium. Biochem. Pharmacol., *252:* 7392–7394, 1995.
11. Kaeck, M., Lu, J., Strange, R., Ip, C., Ganther, H., and Thompson, H. J. Differential induction of growth arrest inducible genes by selenium compounds. Biochem. Pharmacol., *53:* 921–926, 1997.
12. Ganther, H. E. Pathways of selenium metabolism including respiratory excretory products. J. Am. Coll. Toxicol., *5:* 1–5, 1986.
13. Kerr, J. F., Wyllie, A. H., and Currie, A. R. Apoptosis: a basic biological phenomenon with wide-ranging implications in tissue kinetics. Br. J. Cancer., *26:* 239–257, 1972.
14. Earnshaw, W. C., Martins, L. M., and Kaufmann, S. H. Mammalian caspases: structure, activation, substrates, and functions during apoptosis. Annu. Rev. Biochem., *68:* 383–424, 1999.
15. Wolf, B. B., and Green, D. R. Suicidal tendencies: apoptotic cell death by caspase family proteinases. J. Biol. Chem., *274:* 20049–20052, 1999.
16. Martin, D. S., Bertino, J. R., and Koutcher, J. A. ATP depletion plus pyrimidine depletion can markedly enhance cancer therapy: fresh insight for a new approach. Cancer Res., *60:* 6776–6783, 2000.
17. Budihardjo, I., Oliver, H., Lutter, M., Luo, X., and Wang, X. Biochemical pathways of caspase activation during apoptosis. Annu. Rev. Cell Dev. Biol., *15:* 269–290, 1999.
18. Li, H., Zhu, H., Xu, C. J., and Yuan, J. Cleavage of BID by caspase 8 mediates the mitochondrial damage in the Fas pathway of apoptosis. Cell, *94:* 491–501, 1998.
19. Luo, X., Budihardjo, I., Zou, H., Slaughter, C., and Wang, X. Bid, a Bcl2 interacting protein, mediates cytochrome *c* release from mitochondria in response to activation of cell surface death receptors. Cell, *94:* 481–490, 1998.
20. Slee, E. A., Keogh, S. A., and Martin, S. J. Cleavage of BID during cytotoxic drug and UV radiation-induced apoptosis occurs downstream of the point of Bcl-2 action and is catalysed by caspase-3: a potential feedback loop for amplification of apoptosis-associated mitochondrial cytochrome *c* release. Cell Death Differ., *7:* 556–565, 2000.
21. Chen, Q., Gong, B., and Almasan, A. Distinct stages of cytochrome *c* release from mitochondria: evidence for a feedback amplification loop linking caspase activation to mitochondrial dysfunction in genotoxic stress induced apoptosis. Cell Death Differ., *7:* 227–233, 2000.
22. Kirsch, D. G., Doseff, A., Chau, B. N., Lim, D. S., de Souza-Pinto, N. C., Hansford, R., Kastan, M. B., Lazebnik, Y. A., and Hardwick, J. M. Caspase-3-dependent cleavage of Bcl-2 promotes release of cytochrome c. J. Biol. Chem., *274:* 21155–21161, 1999.
23. Frisch, S. M., and Francis, H. Disruption of epithelial cell-matrix interactions induces apoptosis. J. Cell Biol., *124:* 619–626, 1994.
24. Jiang, C., Jiang, W., Ip, C., Ganther, H., and Lu, J. Selenium-induced inhibition of angiogenesis in mammary cancer at chemopreventive levels of intake. Mol. Carcinog., *26:* 213–225, 1999.
25. Margolin, N., Raybuck, S. A., Wilson, K. P., Chen, W., Fox, T., Gu, Y., and Livingston, D. J. Substrate and inhibitor specificity of interleukin-1 β-converting enzyme and related caspases. J. Biol. Chem., *272:* 7223–7228, 1997.
26. Lu, J., Kaeck, M., Jiang, C., Wilson, A. C., and Thompson, H. J. Selenite induction of DNA strand breaks and apoptosis in mouse leukemic L1210 cells. Biochem. Pharmacol., *47:* 1531–1535, 1994.
27. Carson, J. P., Kulik, G., and Weber, M. J. Antiapoptotic signaling in LNCaP prostate cancer cells: a survival signaling pathway independent of phosphatidylinositol 3′-kinase and Akt/protein kinase B. Cancer Res., *59:* 1449–1453, 1999.

28. Marte, B. M., and Downward, J. PKB/Akt: connecting phosphoinositide 3-kinase to cell survival and beyond. Trends Biochem. Sci., *22:* 355–358, 1997.

29. Cardone, M. H., Roy, N., Stennicke, H. R., Salvesen, G. S., Franke, T. F., Stanbridge. E., Frisch, S., and Reed, J. C. Regulation of cell death protease caspase-9 by phosphorylation. Science (Washington DC), *282:* 1318–1321, 1998.

30. Datta, S. R., Dudek, H., Tao, X., Masters, S., Fu, H., Gotoh, Y., and Greenberg, M. E. Akt phosphorylation of BAD couples survival signals to the cell-intrinsic death machinery. Cell, *91:* 231–241, 1997.

31. del Peso, L., Gonzalez-Garcia, M., Page, C., Herrera, R., and Nunez, G. Interleukin-3-induced phosphorylation of BAD through the protein kinase Akt. Science (Washington DC), *278:* 687–689, 1997.

32. Ichijo, H. From receptors to stress-activated MAP kinases. Oncogene, *18:* 6087–6093, 1999.

33. Park, H. S., Huh, S. H., Kim, Y., Shim, J., Lee, S. H., Park, I. S., Jung, Y. K., Kim, I. Y., and Choi, E. J. Selenite negatively regulates caspase-3 through a redox mechanism. J. Biol. Chem., *275:* 8487–8491, 2000.

34. Frisch, S. M. Evidence for a function of death-receptor-related, death-domain-containing proteins in anoikis. Curr. Biol., *9:* 1047–1049, 1999.

35. Rytomaa, M., Martins, L. M., and Downward, J. Involvement of FADD and caspase-8 signaling in detachment-induced apoptosis. Curr. Biol., *9:* 1043–1046, 1999.

36. Rytomaa, M., Lehmann, K., and Downward, J. Matrix detachment induces caspase-dependent cytochrome *c* release from mitochondria: inhibition by PKB/Akt but not raf signaling. Oncogene, *19:* 4461–4468, 2000.

37. Tang, D. G., Li, L., Chopra, D. P., and Porter, A. T. Extended survivability of prostate cancer cells in the absence of trophic factors: increased proliferation, evasion of apoptosis, and the role of apoptosis proteins. Cancer Res., *58:* 3466–3479, 1998.

Caspases as Key Executors of Methyl Selenium-induced Apoptosis (Anoikis) of DU-145 Prostate Cancer Cells

Cheng Jiang, Zaisen Wang, Howard Ganther, et al.

Updated version	Access the most recent version of this article at: http://cancerres.aacrjournals.org/content/61/7/3062

Cited articles	This article cites 35 articles, 14 of which you can access for free at: http://cancerres.aacrjournals.org/content/61/7/3062.full#ref-list-1
Citing articles	This article has been cited by 37 HighWire-hosted articles. Access the articles at: http://cancerres.aacrjournals.org/content/61/7/3062.full#related-urls

E-mail alerts	Sign up to receive free email-alerts related to this article or journal.
Reprints and Subscriptions	To order reprints of this article or to subscribe to the journal, contact the AACR Publications Department at pubs@aacr.org.
Permissions	To request permission to re-use all or part of this article, use this link http://cancerres.aacrjournals.org/content/61/7/3062. Click on "Request Permissions" which will take you to the Copyright Clearance Center's (CCC) Rightslink site.